Molecular Biology of the Cell
Vol. 11, 2553–2563, August 2000

Analysis of Cortical Flow Models In Vivo

Hélène A. Benink,* Craig A. Mandato,* and William M. Bement*†‡

*Department of Zoology, and †Program in Cellular and Molecular Biology, University of Wisconsin, Madison, Wisconsin 53706

Submitted January 5, 2000; Revised May 11, 2000; Accepted May 25, 2000
Monitoring Editor: Thomas D. Pollard

Cortical flow, the directed movement of cortical F-actin and cortical organelles, is a basic cellular motility process. Microtubules are thought to somehow direct cortical flow, but whether they do so by stimulating or inhibiting contraction of the cortical actin cytoskeleton is the subject of debate. Treatment of *Xenopus* oocytes with phorbol 12-myristate 13-acetate (PMA) triggers cortical flow toward the animal pole of the oocyte; this flow is suppressed by microtubules. To determine how this suppression occurs and whether it can control the direction of cortical flow, oocytes were subjected to localized manipulation of either the contractile stimulus (PMA) or microtubules. Localized PMA application resulted in redirection of cortical flow toward the site of application, as judged by movement of cortical pigment granules, cortical F-actin, and cortical myosin-2A. Such redirected flow was accelerated by microtubule depolymerization, showing that the suppression of cortical flow by microtubules is independent of the direction of flow. Direct observation of cortical F-actin by time-lapse confocal analysis in combination with photobleaching showed that cortical flow is driven by contraction of the cortical F-actin network and that microtubules suppress this contraction. The oocyte germinal vesicle serves as a microtubule organizing center in *Xenopus* oocytes; experimental displacement of the germinal vesicle toward the animal pole resulted in localized flow away from the animal pole. The results show that 1) cortical flow is directed toward areas of localized contraction of the cortical F-actin cytoskeleton; 2) microtubules suppress cortical flow by inhibiting contraction of the cortical F-actin cytoskeleton; and 3) localized, microtubule-dependent suppression of actomyosin-based contraction can control the direction of cortical flow. We discuss these findings in light of current models of cortical flow.

INTRODUCTION

Cortical flow is the process whereby material in the cell cortex (the outer ~1–5 μm of the cell) is translocated parallel to the plane of the plasma membrane (Bray and White, 1988). Although cortical flow is observed in a variety of cellular motility processes, it is especially striking during cytokinesis, when cortical F-actin (Cao and Wang, 1990), F-actin–binding proteins (Sanger *et al.*, 1994), myosin-2 (DeBiasio *et al.*, 1996), cortical organelles (Scott, 1960; Hird and White, 1993), and cell surface proteins (Koppel *et al.*, 1982; Wang *et al.*, 1994) all converge on the site of the incipient furrow. The extent of cortical flow varies in different systems and under different conditions. Cortical flow can occur over the entire surface of cells or embryos (Hird and White, 1993) or it may be restricted to a defined region of the cell (Wang *et al.*, 1994; Fishkind and Wang, 1996). In either case, the net result is the same, with cortical F-actin, cortical organelles, and cell surface proteins converging on a particular area of the cortex.

‡ Corresponding author. E-mail address: wmbement@facstaff.wisc.edu.

Cortical flow is thought to be important during cytokinesis because evidence suggests that the accumulation of cortical F-actin in the incipient cytokinetic apparatus results from the convergent flow of F-actin from regions adjacent to the furrow (Cao and Wang, 1990). In addition, manipulations of the cytoskeleton that prevent cytokinesis, such as F-actin, myosin-2, or microtubule perturbation, also perturb cortical flow (Fishkind and Wang, 1996; Shelton *et al.*, 1999). Furthermore, inhibition of cortical flow by cross-linking cell surface proteins with high concentrations of lectins also prevents cytokinesis (Tencer, 1978; Geuskens and Tencer, 1979). Therefore, it is widely thought that cortical flow is responsible for the establishment and/or amplification of the cytokinetic apparatus (Bray and White, 1988; Fishkind and Wang, 1995; however, see also Rappaport, 1996; Oegema and Mitchison, 1997).

Because of the well-known relationship between microtubules and cell division in animal cells (Rappaport, 1996), the nature of microtubule effects on cortical flow and contraction of the cortical actomyosin cytoskeleton are of considerable interest (White and Borisy, 1983; Bray and White, 1988; Hird and White, 1993; Foe *et al.*, 2000). However, because in

many systems microtubules are required for the initiation of cortical flow (Fishkind *et al.*, 1996), direct assessment of the impact of microtubules on cortical flow has been problematic. Two studies of flow patterns after microtubule manipulation reached opposite conclusions. Rappaport and Rappaport (1988) found that when microtubule asters are trapped within a starfish embryo constricted into a dumbbell shape, flow moves away from the half of the embryo containing the asters. They concluded that the half containing the asters was more contractile and squeezed cytoplasm into the other half (Rappaport and Rappaport, 1988; Rappaport, 1996). Hird and White (1993), on the other hand, found that, in *Caenorhabditis elegans* embryos treated with nocodazole to create a diminutive aster near the cortex, cortical flow of F-actin moved away from the aster. They concluded that cortical contractility was lowest at this site and that movement was driven by relatively higher contractility at sites distal to the aster.

Thus, the relationship between microtubules, contraction of cortical actomyosin, and cortical flow remains controversial. Previously, we developed the *Xenopus* oocyte as a simple model system for in vivo analysis of cortical flow (Canman and Bement, 1997). In this system, cortical flow is triggered by application of phorbol 12-myristate 13-acetate (PMA) and moves toward the animal pole of the oocyte, as manifested by the redistribution of cortical pigment granules, cortical F-actin, and cell surface proteins. The *Xenopus* oocyte system has several distinct advantages for cortical flow analysis. First, because flow is inducible and can be followed by observation of the pigment margin, rates of flow can be easily quantified under a variety of experimental conditions. Second, the large size of the oocyte (~1.2 mm in diameter) permits physical manipulations impossible in other systems. Third, the predictable nature of the normal cortical flow pattern permits straightforward interpretation of results after manipulation of microtubules.

Here, the oocyte system was used to test the basic tenets of cortical flow models. Using physical and pharmacological manipulations in combination with confocal fluorescence analysis of fixed samples as well as time-lapse, confocal fluorescence (4D) analysis, we provide the first direct demonstration that global cortical flow is directed toward sites of localized contraction of the cortical F-actin cytoskeleton. We also demonstrate that flow itself is driven by contraction of the cortical F-actin cytoskeleton and that microtubules slow flow by inhibiting this contraction. Finally, we show that cortical flow is directed away from displaced microtubule organizing centers.

MATERIALS AND METHODS

Procurement, Storage, and Treatment of Oocytes

Procurement and storage of oocytes as well as stock solutions were as described previously (Canman and Bement, 1997). With the exception of the live imaging experiments, all oocytes were transferred directly into fix solution after the manipulations described below. Oocytes in each experiment were obtained from the same frog, and no two experiments testing the same phenomenon were done with oocytes from the same frog (e.g., each redirection experiment was done with oocytes from different frogs).

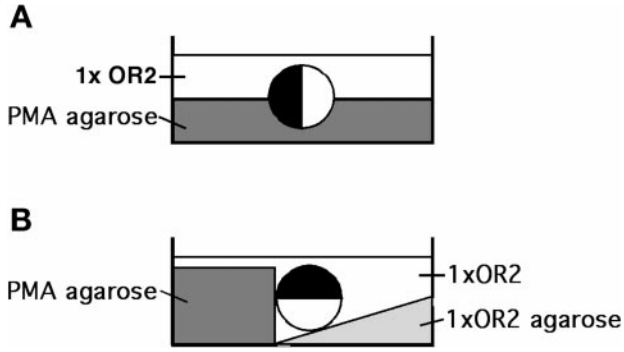

Figure 1. Schemes showing the methods by which cortical flow was redirected and ectopic furrows were induced. (A) Method used to redirect cortical flow. The oocyte (shown on its side) is positioned in a bed of PMA-containing agarose such that approximately half of the oocyte surface is in contact with PMA. (B) Method used to induce ectopic furrows. The oocyte is positioned and held against PMA-containing agarose with the slope of agarose lacking PMA such that only a very localized area on the oocyte surface is in contact with PMA.

Redirection of Flow

For redirection of cortical flow, Petri dishes containing PMA–agarose were prepared by heating 1% agarose in 1× OR2 buffer (82.5 mM NaCl, 2.5 mM KCl, 1 mM $CaCl_2$, 1 mM $MgCl_2$, 1 mM Na_2HPO_4, 5 mM HEPES, pH 7.4), cooling to ~50°C, and then supplementing with PMA (Calbiochem, San Diego, CA) at a final concentration of 300 nM. After the addition of PMA, the molten PMA–agarose mixture was quickly poured into Petri dishes and allowed to set. 1× OR2 buffer was poured over the hardened PMA–agarose, and small circular indentations were made in the PMA–agarose with the use of a small (1.2–1.4 mm in diameter) glass ball mounted on a capillary tube. These indentations were approximately the diameter of an oocyte in width and the radius of an oocyte in depth. Defolliculated oocytes were positioned in the indentations with the animal hemisphere, vegetal hemisphere, or side facing the agar (Figure 1A), and they were allowed to remain undisturbed for 1–1.5 h, depending on how well control oocytes subjected to 50 nM PMA flowed (see Canman and Bement, 1997). For determination of the effects of microtubule depolymerization on redirected flow by 180 degrees, oocytes were pretreated with 660 nM nocodazole for 1 h and then positioned in PMA–agarose as described above.

Ectopic Furrow Formation

To induce ectopic furrow formation, 1% agarose made with the use of 1× OR2 buffer was poured into Petri dishes that were positioned at an angle such that the agarose formed a slope with respect to the bottom of the dish. These were allowed to set for at least 1 h. The dishes were then positioned flat on the bench top, and a sheet of thin plastic cut to fit over the agar in each dish was put in place and 1% agarose containing 300 nM PMA was poured over the plastic. The plastic sheet prevented the PMA from diffusing into the angled agar below. After the PMA-containing agar set, a razor blade was used to cut vertically through this agar and the plastic was removed. 1× OR2 was poured into the dish, and defolliculated oocytes were positioned in the dish along the cut edge of PMA-containing agar (Figure 1B). These were allowed to stay in place undisturbed for 2 h.

Germinal Vesicle Displacement

To displace the germinal vesicles toward the animal pole, defolliculated oocytes were positioned animal hemisphere up between two

nylon meshes in a Petri dish containing 1× OR2. The meshes were held in place with clay. The dishes were placed at 4°C for 1–1.5 h to depolymerize microtubules and allow for the germinal vesicle (GV) migration to occur (this protocol is a modification of one developed by Gard [1993] for GV displacement). Oocytes that showed depigmentation at the animal pole after incubation at 4°C were not used for analysis. After incubation at 4°C, oocytes were allowed to recover at room temperature for 3 h to allow microtubules to repolymerize. Oocytes were then removed from the mesh, and cortical flow was induced by global exposure to 50 nM PMA.

Fluorescent Microscopy of Fixed Oocytes

Actin Filaments and Myosin-2

After a given manipulation, oocytes were fixed for 4 h in splooge buffer: 80 mM K–piperazine-*N*,*N*′-bis[2-ethanesulfonic acid], pH 6.8, 5 mM EGTA, 1 mM $MgCl_2$, 0.2% Triton X-100 containing 3.7% paraformaldehyde (Bement *et al.*, 1999). After three or four rapid washes, the oocytes were rocked overnight in Tris-buffered saline containing 0.1% NP-40 (TBSN). Oocytes were then stained for F-actin overnight in TBSN containing 5% DMSO plus 1.5 U/ml Texas Red–X-phalloidin (Molecular Probes, Eugene, OR). Oocytes were then washed for 12–24 h in TBSN and mounted. For the double staining of F-actin and myosin-2, oocytes were fixed as described above, washed for a minimum of 12 h, and placed in TBSN plus 10 mg/ml BSA for 1 h at 4°C with gentle rocking. Oocytes were then stained for 20–24 h at 4°C with gentle rocking in TBSN/BSA containing Texas Red–X-phalloidin at 1.5 U/ml plus 1 μg/ml affinity-purified anti-*Xenopus* nonmuscle myosin-IIA antibody (a generous gift from Dr. Robert "The Chopper" Adelstein, National Institutes of Health, Bethesda, MD) at 1:500. Oocytes were washed at 4°C for 40–48 h in TBSN/BSA with gentle rocking and analyzed on a Bio-Rad (Richmond, CA) 1024 laser scanning confocal microscope.

Microtubules

For visualization of microtubules, oocytes were fixed and stained as described by Gard (1991). Briefly, oocytes were fixed for 4 h in splooge buffer with 0.25% glutaraldehyde plus 0.5 μM taxol (Cytoskeleton, Denver, CO). Oocytes were postfixed overnight in −20°C methanol, rehydrated in PBS, and incubated overnight in PBS plus 100 mM $NaBH_4$. Oocytes were rinsed for 4–6 h in TBSN, bisected, and incubated overnight at 4°C in TBSN plus 2 mg/ml BSA plus DM1A (monoclonal anti-tubulin antibody; ICN Biochemicals, Costa Mesa, CA) at 1:250 with gentle rocking. Oocytes were washed overnight in TBSN at 4°C with gentle rocking and incubated overnight in TBSN/BSA plus rhodamine-labeled goat anti-mouse antibody (Organon Teknika, Fanningsanus, PA) at 1:100. Oocytes were then washed overnight at 4°C in TBSN, dehydrated in methanol, cleared in benzyl benzoate–benzyl alcohol, mounted, and examined as described above.

Flow Rate Analysis

Flow rate of the pigment margin was measured and calculated as described previously (Canman and Bement, 1997) with some modifications necessitated by the induced backward flow (180 degrees to normal). Two measurements (made with an ocular micrometer) were used to calculate the rate of flow in oocytes. The first measurement, made before PMA addition, was the diameter of each of 10 oocytes in a group. Each group represented a different orientation on the agar and/or drug treatment. The second measurement, Z, was taken for each oocyte after exposure to PMA and fixation. Z represents the distance from the pigment margin to the vegetal pole minus the radius. The rate of cortical flow for oocytes that flowed toward the animal pole was calculated with the use of the formula for a shrinking cap on a sphere [rate = $-2\pi R(\partial Z/\partial t)$], and the opposite formula [rate = $+2\pi R(\partial Z/\partial t)$] was used for those oocytes that flowed toward the vegetal pole. Because the absolute rate of cortical flow varied from batch to batch, all measurements were standardized to the calculated rate of a control group from the same batch of oocytes (i.e., cortical flow rates are expressed as a percentage of the flow rate of a group of oocytes that were only bathed in 50 nM PMA). All pigment images were obtained with the use of a video microscope with oocytes positioned on a nylon mesh to immobilize them during filming.

4D Live Imaging

Oocytes were injected in the equatorial region with ~30 nl of either Texas Red–X-phalloidin at 3 U/ml or X-rhodamine–actin (a generous gift from Dr. Clare Waterman-Storer, Scripps Research Institute, La Jolla, CA) at 3 mg/ml with the use of a PLI-100 Pico-Injector (Medical Systems, Greenvale, NY). Oocytes injected with phalloidin were recovered in 0.5% BSA/1× OR2 for >7 h to allow for adequate incorporation, whereas actin-injected cells required only a 4-h incorporation time. For microtubule modulation, oocytes were preincubated for 1 h in 20 μM nocodazole or 25 μM taxol immediately before 4D analysis and then imaged with the same concentrations of these drugs in the imaging chamber. Longer incubation times were undesirable for nocodazole treatment, because this occasionally resulted in displacement of the GV to the animal pole. With a 1-h incubation in nocodazole followed by ~1 h of imaging in the presence of nocodazole, GV displacement to the animal pole generally did not occur, presumably because oocytes were oriented upside down for 4D analysis, which would result in the GV being displaced toward the vegetal pole (Gard, 1993).

Oocytes were imaged in chambers consisting of a small nylon mesh held in place with clay above a 22 × 22 mm coverslip that covered and sealed a hole made in the bottom of a small Petri dish. All 4D imaging was performed with a Zeiss (Thornwood, NY) Axiovert 100 M microscope with the Bio-Rad 1024 Lasersharp Confocal package, with the use of a 10× objective and a laser power of 1%. After a 10-min preincubation in 300 nM PMA in 1× OR2 to stimulate cortical flow, a single oocyte was placed in an imaging chamber containing 300 nM PMA. Once the oocyte was positioned in the chamber, imaging was begun either immediately or after photobleaching of a 150 × 150 μm square on the cortex of the oocyte. Photobleaching consisted of 7–10 slow scans at 100% laser power. The number of scans varied because of differences in the time it took for injected material to incorporate into the cortex. Three-dimensional stacks of confocal fluorescence images were taken every 2 min for 1 h. A 4D movie was then constructed from the confocal stacks, and analysis of flow and shrinkage rates was done with the use of NIH Image 1 software.

RESULTS

Cortical Flow Can Be Redirected by Localized Application of the Contractile Stimulus

Oocytes display cortical flow toward the animal pole when globally treated with PMA (Canman and Bement, 1997). To determine whether cortical flow could be redirected toward a localized contractile stimulus, oocytes were positioned in depressions made in agarose containing PMA (Figure 2). Localized application of PMA redirected cortical flow such that pigment in oocytes oriented with their equators against PMA–agarose displayed translocation toward the side of the oocyte facing the agarose (90 degrees from normal), whereas oocytes oriented with their vegetal poles facing the PMA–agarose displayed pigment translocation toward the vegetal pole (180 degrees from normal; Figure 2).

To determine whether redistribution of cortical pigment granules was accompanied by redistribution of actomyosin,

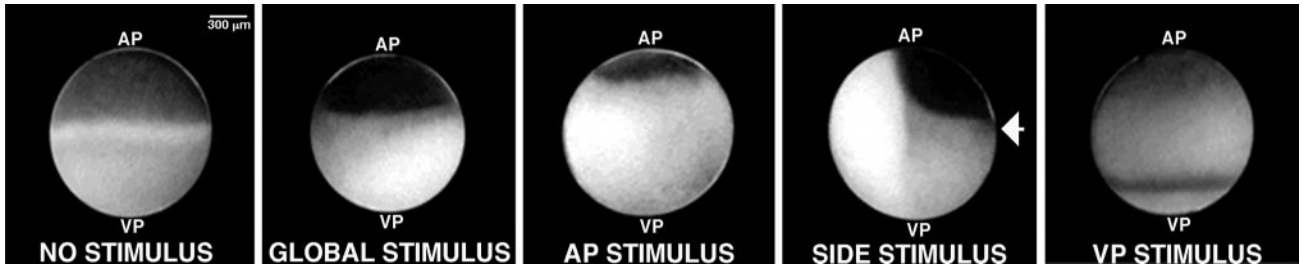

Figure 2. Localized contractile stimulus redirects the flow of cortical pigment granules toward the site of application. Controls show pigmentation before the addition of PMA (no stimulus) and the preprogrammed cortical flow of pigment granules resulting from global application of PMA (global stimulus). In oocytes subjected to the localized application of PMA to the animal pole region (AP stimulus), the side (side stimulus; applied on the right side of the oocyte), and the vegetal pole region (VP stimulus), cortical flow is revealed by the movement of pigment granules toward the region of stimulus.

samples were fixed and stained for cortical F-actin and myosin-2. In control (untreated) oocytes, F-actin is uniformly distributed over the surface of the oocyte (Figure 3A). Myosin-2 appears to be more abundant in the vegetal hemisphere of control oocytes; however, immunoblot analysis of bisected oocytes indicates that more myosin-2 is present in the animal hemisphere (our unpublished results), suggesting that the opaque pigment granules of the animal hemisphere obscure the myosin-2 signal in this region of untreated oocytes. In oocytes oriented animal hemisphere down on agarose–PMA, both cortical F-actin and myosin-2 show an accumulation at the animal pole (Figure 3A), whereas oocytes oriented with their vegetal poles facing the PMA–agarose displayed accumulations of cortical F-actin and myosin-2 at their vegetal poles (Figure 3A). Thus, cortical flow of F-actin and myosin-2 can be redirected by 180 degrees in response to a localized contractile stimulus. Furthermore, localized contraction of the cortical actomyosin cytoskeleton was capable of triggering furrow formation when PMA was applied to a more restricted portion of the oocyte surface. This manipulation resulted in ectopic, F-actin–rich furrows at the site of PMA application (Figure 3B).

Effects of Global Microtubule Manipulation on Contraction of the Cortical F-Actin Cytoskeleton and Cortical Flow

Microtubule depolymerization accelerates cortical flow toward the animal pole (Canman and Bement, 1997). To determine whether it has the same effect on redirected flow, oocytes were preincubated in nocodazole for 1 h and then positioned on PMA–agarose with their vegetal poles facing the agarose to induce backward (i.e., 180-degree redirected) flow. This manipulation resulted in a near doubling of cortical flow rate relative to the rate in control oocytes undergoing backward flow (189 ± 2% of control rate [mean ± SEM, n = 3]). Thus, suppression of cortical flow by microtubules is independent of the direction of cortical flow.

To directly observe and quantify the effects of microtubule manipulation on cortical F-actin, oocytes were injected with X-rhodamine–actin, treated with PMA to trigger cortical flow, and then analyzed by 4D microscopy. In control oocytes (those not subjected to microtubule manipulation), PMA application triggered flow of cortical F-actin toward the animal pole, as observed by movement of a photo-

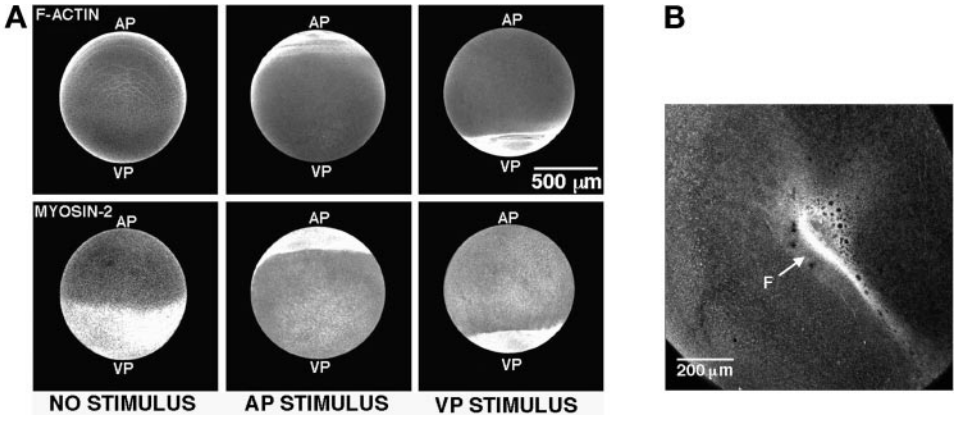

Figure 3. Distribution of F-actin and myosin-2 after redirected flow. (A) Cortical F-actin and myosin-2 accumulate at sites of localized contractile stimulus. Confocal fluorescence images of F-actin stained with Texas Red–X-phalloidin and immunolabeled myosin-2 in oocytes that have undergone redirected cortical flow. In contrast to controls (no stimulus), oocytes that were positioned with either their animal poles (AP stimulus) or vegetal poles (VP stimulus) facing the PMA-containing agarose show an enrichment of both F-actin and myosin-2 at the animal pole or vegetal pole, respectively. (B) Confocal fluorescence image of an ectopic furrow on an oocyte stained with Texas Red–X-phalloidin. The furrow (F) is rich in F-actin.

bleached area on the oocyte surface or by analysis of the movement of individual F-actin aggregations (Figure 4, A and B). Microtubule depolymerization by nocodazole treatment more than doubled the rate of movement of cortical F-actin relative to controls, whereas taxol treatment slowed the movement of cortical F-actin by slightly more than half relative to controls (Figure 4, C–E). The suppression of cortical F-actin movement by microtubules was also observed when Texas Red–X-phalloidin was used as a marker (Figure 4E). The use of the former ensures that F-actin dynamics are not perturbed by the introduction of phalloidin into the oocyte, whereas the use of the latter ensures that movement of F-actin rather than complexes of unpolymerized actin (Cao *et al.*, 1993; Hird, 1996) are being observed.

We previously proposed that PMA-induced flow is powered by contraction of the cortical actomyosin network, based on the fact that it is sensitive to pharmacological inhibition of myosins (Canman and Bement, 1997). If this were correct, photobleached areas would shrink in time and the rate of shrinkage would be proportional to the overall flow rate. Plotting of flow rates versus shrinkage rates for untreated oocytes, PMA-treated oocytes, and nocodazole-treated oocytes confirmed this notion (Figure 4F). Furthermore, nocodazole increased shrinkage of photobleached areas, whereas taxol reduced shrinkage, relative to controls (Figure 4F). Thus, microtubules suppress cortical flow by suppressing contraction of the cortical actomyosin cytoskeleton.

Cortical Flow Moves Away from Repositioned GVs

These results showed that microtubules globally suppress contraction of the cortical F-actin cytoskeleton and cortical flow, regardless of the direction of flow. To determine whether this suppression was capable of controlling the direction of flow, we sought to manipulate the distribution of microtubules and then analyze the effects of such manipulations on globally induced cortical flow. We modified an approach developed by Gard (1993) to displace the oocyte GV (i.e., the nucleus). In *Xenopus* oocytes, the GV serves as a microtubule organizing center (Gard, 1991). The GV can be experimentally repositioned close to the animal pole by exposing oocytes to cold shock, after which the relatively light GV migrates upward as a result of prolonged microtubule depolymerization (Gard, 1993). After warming, microtubules repolymerize around the displaced GV such that microtubule density near the animal pole is much greater than in control oocytes (Figure 5A).

After GV repositioning, oocytes were induced to undergo normal cortical flow by global application of PMA. Displacing the GV toward the animal pole resulted in local disruption of the normal pattern of cortical flow at the animal pole. Specifically, cortical pigment granules moved centrifugally away from the animal pole, resulting in localized clearing of pigment granules at the top of the oocyte (Figure 5B). Confocal fluorescence analysis of F-actin and myosin-2 distribution in such oocytes demonstrated that actomyosin accumulates around the circumference of the oocyte in a ring positioned between the equator and the animal pole (Figure 5B). Circumferential indentations or furrows in the oocyte surface were often seen in the same position as the actomyosin accumulation in oocytes subjected to GV displacement (our unpublished results).

The circular accumulation of actomyosin and pigment granules in oocytes subjected to GV displacement was most easily explained by the convergence of cortical flow from two directions: the "preprogrammed" flow toward the animal pole, and experimentally induced flow away from repositioned GV. To test this possibility directly, oocytes were injected with Texas Red–X-phalloidin as described above and then subjected to GV displacement to the animal pole. After allowing sufficient time for microtubule repolymerization, oocytes were treated with PMA to trigger cortical flow and analyzed by 4D microscopy to track the movement of cortical F-actin.

Before the onset of flow, F-actin was distributed uniformly throughout the oocyte cortex (Figure 6A). After treatment with PMA to induce flow, the previously described movement of F-actin from the vegetal hemisphere toward the animal pole was observed by following the movement of F-actin aggregations over time. However, in addition to this pattern of flow, a second pattern was observed wherein cortical F-actin moved centrifugally away from the animal pole. This movement resulted in the formation of a circular area of low actin signal around the position of the displaced GV (Figure 6A, arrowheads). The edge of this circular area developed into the site of an intense accumulation of F-actin (Figure 6A, arrows). Higher-magnification views showed that the flow of F-actin away from the displaced GV converged with F-actin moving toward the animal pole from the vegetal half of the oocyte in this area (Figure 6, B and C). At later times in the analysis (50–90 min after the onset of flow), the circumferential F-actin arrays either remained stationary above the oocyte equator or moved back toward the animal pole while undergoing circumferential shrinkage. This eventual movement of the arrays is presumably the result of the "hard-wired" flow overcoming flow away from the repositioned GV, the actomyosin-based contraction of the circumferential arrays themselves, or both.

Simultaneous preservation of both F-actin and microtubules in *Xenopus* oocytes has proven impossible to date (Gard *et al.*, 1995), which prevented us from comparing the distribution of microtubules to actomyosin in oocytes subjected to GV displacement. Therefore, to ensure that the redirection of flow resulted from microtubules, rather than from the GV simply displacing the cortical F-actin network or some other effect of the experimental protocol, two precautions were taken. First, oocytes in which the GV had migrated too close to the cortex (as demonstrated by pigment of F-actin clearing from the animal pole before the induction of cortical flow by PMA treatment) were excluded from analysis. Second, in parallel with the above analysis, a subset of the oocytes subjected to GV repositioning was treated with nocodazole before cortical flow induction. Nocodazole treatment significantly reduced the redirection of cortical flow that accompanied GV repositioning (Figure 7), demonstrating that the observed pattern of cortical pigment and actomyosin accumulation in circumferential arrays is, in fact, microtubule-dependent.

DISCUSSION

The goal of this work was to empirically evaluate models of cortical flow by exploiting the *Xenopus* oocyte system. We cannot be certain that our findings are relevant to cytokine-

sis or other phenomena involving cortical flow, although the striking similarity of cytokinesis to cortical contractile processes in amphibian eggs has been noted by a number of different investigators in earlier studies (Gingell, 1970; Bluemink, 1972; Schroeder and Strickland, 1974; Merriam and Christensen, 1983). Schroeder (1975) in particular emphasized the importance of obtaining a detailed understanding of amphibian egg contraction as a means to better un-

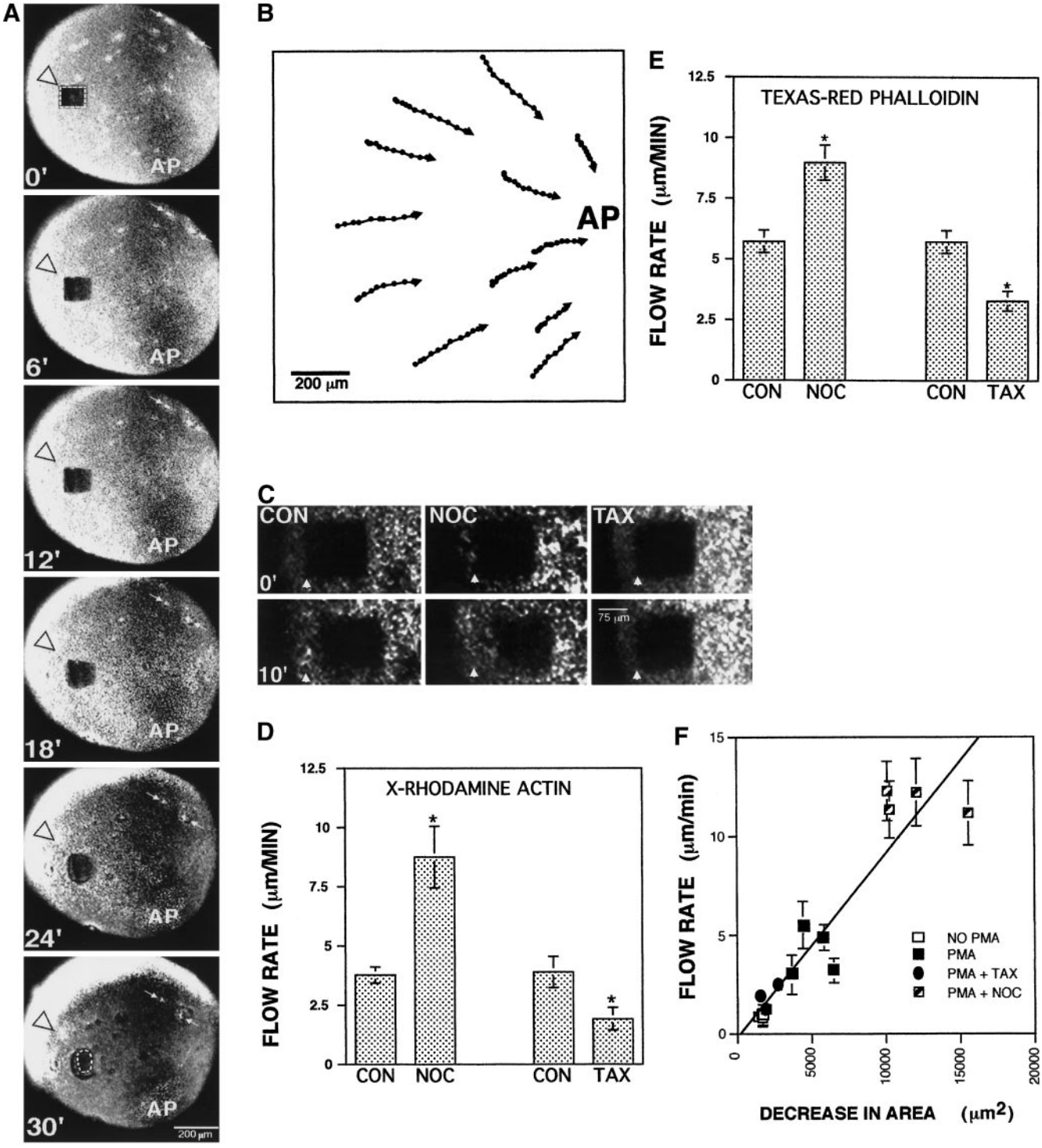

Figure 4.

derstand cytokinesis. Toward this end, in a previous study (Canman and Bement, 1997) and in the present study, we have characterized the basic features of PMA-induced cortical flow in the oocyte system and compared them with cortical flow during cytokinesis. Cortical flow in the oocyte system occurs on a global scale, but it is otherwise remarkably similar to cortical flow in other systems in that it entails convergent movement of cortical organelles, cortical F-actin, cortical myosin-2, and cell surface proteins; it is sensitive to perturbation of F-actin and myosin-2; it is sensitive to high concentrations of extracellular lectins; it is tightly regulated by microtubules; and it is capable of producing furrows. Thus, PMA-induced oocyte cortical flow is not only similar to cortical flow in other systems in terms of morphology but actually uses the same downstream players.

We do not yet know the upstream players that trigger contraction of cortical actomyosin in the oocyte cortical flow system. Presumably, the first step is PKC activation, because PMA activates PKCs and a variety of evidence shows that PKC is responsible for coupling calcium increases in *Xenopus* oocytes and eggs to cytoskeletal events characteristic of *Xenopus* egg activation (Bement and Capco, 1989; Canman and Bement, 1997; Stith *et al.*, 1997; Taunton *et al.*, 2000). How PKC activation is then converted to contraction of the cortical actomyosin cytoskeleton is unclear. A recent report has demonstrated that treatment of *Xenopus* eggs with PMA results in WASP- and Cdc42-dependent activation of vesicle motility resembling *Listeria*-triggered F-actin "comets" (Taunton *et al.*, 2000). These comets are propelled shark-like through the cytoplasm by de novo actin polymerization and can be easily distinguished from F-actin undergoing cortical flow based on a variety of criteria: comets are isolated and comet-shaped, whereas flowing F-actin is composed of interconnected F-actin aggregates; comets move at 10 μm/min, whereas flowing F-actin moves at 3–5 μm/min; comets move in a curved manner and adjacent comets move randomly with respect to the egg polarity, whereas flowing F-actin moves for long distances in straight lines toward the animal pole; comets do not colocalize with myosin-2, whereas flowing F-actin does; comets do not fuse with each other to give rise to arrays of F-actin hundreds of micrometers long that coincide with furrows; and comets and flow have totally different pharmacological profiles with respect to both PMA and myosin inhibitors (Canman and Bement, 1997; Taunton *et al.*, 2000, this report; A.M. Sokac and W.M. Bement, unpublished results).

Although it is certainly possible that in our study PMA triggered Cdc42 activation, and Cdc42 has been shown to be required for *Xenopus* cytokinesis (Drechsel *et al.*, 1997), there are several differences between the present work and the study by Taunton *et al.* (2000). First, we used oocytes rather than eggs. The two cells, although contained within the same developmental continuum, are distinctly different in a variety of ways (reviewed by Bement, 1992). Second, cortical flow is triggered by 50 nM PMA, whereas 1–2 μM PMA (20–40 times greater) is required for comet formation (Taunton *et al.*, 2000). Thus, if flow is somehow triggered by PMA-dependent Cdc42 activation, the level of Cdc42 activity required is apparently much lower than that required for comet formation.

Theoretical models of cortical flow assume that cortical actomyosin is laterally mobile, that flow is powered by contraction of the cortical actomyosin cytoskeleton, and that it moves toward regions of relatively high cortical contractility (White and Borisy, 1983; Bray and White, 1988). The results of this study confirm the basic tenets of these models. As seen previously for cortical flow of F-actin during cytokinesis (see INTRODUCTION) and for cortical flow during pseudocleavage in *C. elegans* (Hird, 1996), we find by 4D analysis that F-actin moves laterally toward the animal pole in oocytes bathed in PMA.

More interestingly, we were also able to confirm the two other basic tenets of cortical flow theory. First, the 4D photobleaching analysis demonstrates that cortical flow is indeed powered by contraction of the cortical actomyosin network, as shown by the inward shrinkage of photobleached squares on the oocyte surface and by the fact that the degree of this shrinkage is proportional to the rate of F-actin flow. Second, cortical F-actin, cortical myosin-2, and cortical pigment granules flow toward regions of experimentally increased contractility, even when such regions are

Figure 4 (facing page). Microtubules suppress contraction of the cortical F-actin network and flow of cortical F-actin. (A) Low-magnification 4D microscopy analysis of an oocyte injected with X-rhodamine–actin showing the flow of cortical F-actin to the animal pole (AP) of an oocyte bathed in PMA. The dark square (outlined with a dashed line) is a photobleached area that moves toward the animal pole over time. The arrowhead indicates the original position of the upper left corner of the photobleached area. Individual accumulations of cortical F-actin (arrows) can also be seen to move toward the animal pole over time. (B) Vector diagram showing the paths of 12 individual F-actin aggregates over time in an oocyte induced to undergo animal pole–directed cortical flow by global treatment with PMA. Aggregate positions were determined every 2 min. All aggregates flow toward the animal pole. (C) Higher-magnification 4D views of photobleached area movement in control oocytes (CON), oocytes treated with nocodazole (NOC), and oocytes treated with taxol (TAX). Arrowheads indicate the initial starting position of the lower left corner of the photobleached area. Movement of the photobleached area is fastest in nocodazole-treated oocytes and slowest in taxol-treated oocytes. (D) Quantification of F-actin cortical flow rates as determined by 4D analysis of oocytes injected with X-rhodamine–actin and then subjected to microtubule manipulations. Nocodazole more than doubles the rate of F-actin cortical flow, whereas taxol reduces the rate by slightly more than half. Results represent means ± SEM of four independent experiments. The asterisk indicates a p value < 0.05. (E) Quantification of F-actin cortical flow rates as determined by 4D analysis of oocytes injected with Texas Red–X-phalloidin and then subjected to microtubule manipulations. Nocodazole nearly doubles the rate of F-actin cortical flow, whereas taxol reduces the rate by slightly less than half. Results represent means ± SEM of four independent experiments. The asterisk indicates a p value < 0.05. (F) Microtubules suppress contraction of the cortical F-actin network. Rates of F-actin cortical flow plotted versus shrinkage of photobleached areas in oocytes injected with X-rhodamine–actin and then subjected to no treatment (NO PMA), PMA treatment (PMA), PMA treatment after a taxol pretreatment (PMA + TAX), or PMA treatment after a nocodazole pretreatment (PMA + NOC). The rate of cortical flow is proportional to the shrinkage of photobleached areas. PMA plus nocodazole treatment results in increased shrinkage of photobleached areas relative to PMA alone, whereas PMA plus taxol treatment results in decreased shrinkage relative to PMA alone. Virtually no shrinkage (and no cortical flow) is observed in the absence of PMA. Each data point is from a different oocyte; error bars represent means ± SEM of five different cortical flow rate measurements taken for each oocyte.

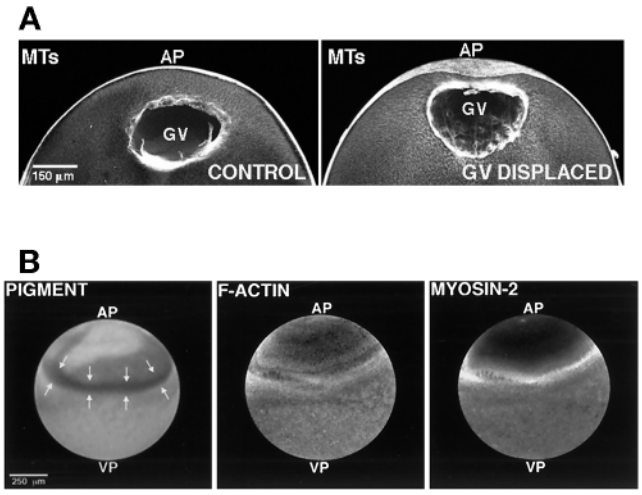

Figure 5. Redirection of cortical flow by GV displacement. (A) Displacement of the oocyte GV toward the animal pole (AP). Confocal immunofluorescence micrographs of microtubule distribution in a control oocyte and an oocyte subjected to displacement of the GV toward the animal pole before the induction of cortical flow. The GV and its associated microtubules (MTs) are in closer proximity to the animal pole in the oocyte subjected to GV displacement. (B) Cortical pigment, F-actin, and myosin-2 distribution after cortical flow in an oocyte with a displaced GV. Cortical pigment granules, F-actin, and myosin-2 are sparse in the area of the animal pole (AP) toward which the GV was displaced. Instead, they accumulate in a ring positioned between the equator and the animal pole of the oocyte. VP, vegetal pole.

on the opposite side of the oocyte to which flow is normally directed. These results are consistent with earlier findings of Schroeder and Strickland (1974), who reported that localized application of calcium ionophore to *Xenopus* eggs caused transient contractions that manifested as pigment accumulation at the site of application. It is likely that the pigment accumulation observed by Schroeder and Strickland (1974) was driven by cortical actomyosin; however, the means to demonstrate this were not available at the time. Moreover, the fact that localized ionophore application induced only a transient cortical contraction would likely have precluded global recruitment of cortical actomyosin to the site of application.

These findings provide direct empirical support for theoretical models of cortical flow that assume that contraction of a cortical F-actin network can power the movement of F-actin and cortical pigment granules parallel to the plane of the plasma membrane. They also provide direct empirical support for the assumption that convergent cortical flow, triggered by localized differences in contraction of the cortical actomyosin cytoskeleton, is sufficient to induce furrowing. In addition, as described below, they provide information crucial for evaluating the role of microtubules in regulating contraction of the cortical actomyosin network and directing cortical flow.

Two distinct lines of evidence from this study show that microtubule-based inhibition of actomyosin-dependent contraction is best able to explain the effects of microtubules on cortical flow in the oocyte system. The first is provided by the quantification of F-actin flow rates and shrinkage of photobleached spots under conditions of microtubule manipulation. Depolymerization of microtubules by nocodazole roughly doubles the rate of F-actin movement relative to that in controls and results in a corresponding increase in the shrinkage of photobleached areas. In contrast, increasing oocyte microtubule levels by taxol treatment roughly halves the rate of F-actin movement and reduces shrinkage of photobleached areas. Because we have shown previously that oocyte cortical flow is myosin-dependent (Canman and Bement, 1997) and have shown here directly that this flow is powered by contraction of the cortical F-actin network, we conclude that global decreases or increases in microtubule levels result in globally increased or decreased actomyosin-based contraction, respectively.

The second line of evidence excludes the possibility that microtubules per se might have a localized stimulatory effect on cortical actomyosin that is distinct from their apparent global inhibitory effect on the contraction of cortical actomyosin during cortical flow in the oocyte system. Namely, we found that flow of F-actin, myosin-2, and cortical pigment granules is directed away from displaced GVs, which serve as microtubule organizing centers in oocytes (Gard, 1991). The localized, redirected flow converges with preprogrammed flow directed toward the animal pole from the vegetal hemisphere, causing the accumulation of actomyosin around the circumference of the oocyte. In the absence of any other information, it could be argued that flow away from the displaced GV resulted from increased cortical contractility squeezing cytoplasm away from the GV. However, our demonstration that cortical flow is directed toward sites of localized contractility excludes this possibility. If microtubules stimulated localized contractility, displacement of the GV toward the animal pole of the oocyte should have accelerated cortical flow toward this region, resulting in accumulation of F-actin, myosin-2, and cortical pigment granules at the animal pole. Instead, the opposite pattern of cortical flow was observed, showing that microtubules do in fact locally inhibit contraction of cortical actomyosin. Thus, our results support the conclusion of Hird and White (1993) that localized inhibition of actomyosin by microtubules results in cortical flow being directed away from asters.

The localized inhibition of actomyosin-based contractility by microtubules observed here is consistent with the repeated demonstration that global microtubule depolymerization stimulates actomyosin-based contractility in cultured cells (Lyass *et al.*, 1988; Danowski, 1989; Kolodney and Elson, 1995; Bershadsky *et al.*, 1996; Liu *et al.*, 1998). It is also consistent with the observation that microtubule depolymerization accelerates the progression of cytokinetic furrows in cultured cells (Hamilton and Snyder, 1983) and the closure of ectopic actomyosin purse strings in *Xenopus* oocytes (Bement *et al.*, 1999). Although the means by which microtubules suppress contraction of cortical actomyosin are not well characterized, several possibilities are suggested by the literature (for review, see Mandato *et al.*, 2000). For example, depolymerization of microtubules results in rho activation (Ren *et al.*, 1999), which is coupled to increased contractility via rho-dependent, kinase-mediated increases in myosin-2 regulatory light chain phosphorylation (Kimura *et al.*, 1996). In addition, it has been proposed that microtubules promote closure of the cytokinetic furrow by directing insertion of membranous vesicles in regions flanking the

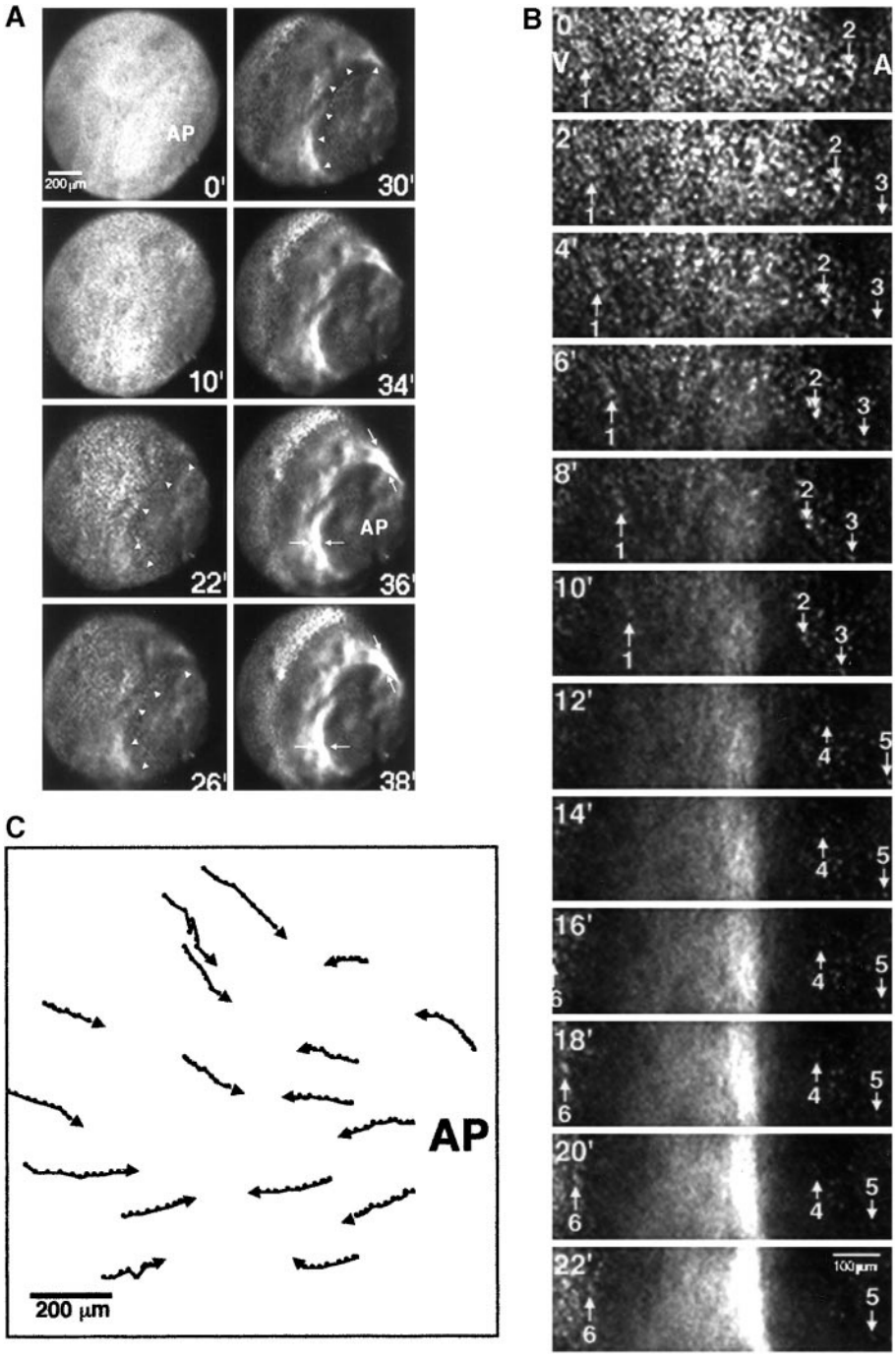

Figure 6. Circumferential rings of F-actin form in oocytes with displaced GVs as a result of convergent cortical flow. (A) Low-magnification 4D analysis of an oocyte injected with Texas Red–X-phalloidin, subjected to GV displacement, and then induced to undergo cortical flow by global treatment with PMA. Initially, F-actin is uniformly distributed throughout the oocyte cortex. After the onset of cortical flow, an F-actin–poor region (the borders of which are indicated by arrowheads) is evident in the region of the animal pole (AP) to which the GV has been displaced. F-actin continues to accumulate at the borders of this region until it is visible as an intense, linear array that encircles the oocyte. (B) High-magnification 4D analysis of convergent cortical flow from the same oocyte shown in A. Six individual F-actin accumulations (indicated by numbers and arrows) flow toward each other as a result of cortical flow away from the vegetal pole (the direction of which is indicated by a V) or away from the animal pole (the direction of which is indicated by an A). Over time, this convergent cortical flow gives rise to an intense, linear accumulation of cortical F-actin. (C) Vector diagram showing the paths of 17 individual F-actin aggregates over time in an oocyte subjected to GV displacement and then induced to undergo cortical flow by global treatment with PMA. Aggregate positions were determined every 2 min. Aggregates in the vegetal hemisphere flow toward the animal pole, whereas aggregates near the animal pole (AP) flow away from the animal pole.

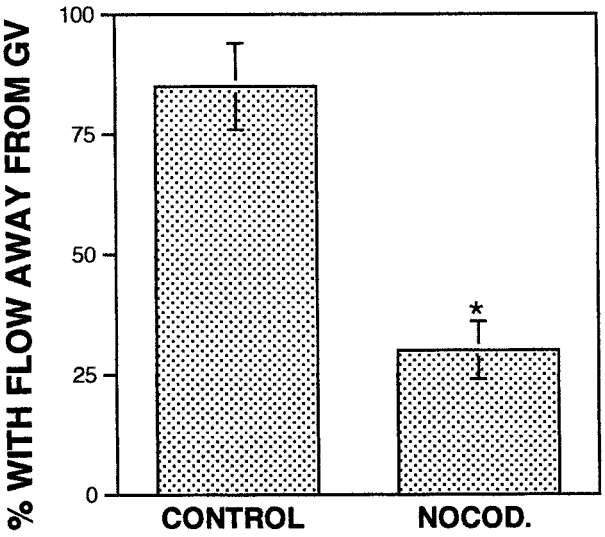

Figure 7. Cortical flow away from displaced GVs is microtubule-dependent. Oocytes were subjected to GV displacement toward the animal pole and then induced to undergo cortical flow in the absence (CONTROL) or presence (NOCOD.) of nocodazole. Redirected cortical flow was judged by observing oocyte pigmentation. Nocodazole significantly reduced the number of oocytes exhibiting cortical flow away from the newly positioned GV. Results are means ± SEM from three independent experiments. The asterisk indicates a p value < 0.05.

cytokinetic furrow (Drechsel *et al.*, 1997; Danilchik *et al.*, 1998), decreasing contractility in such regions by reducing the local concentration of cortical actomyosin. Finally, microtubules might regulate cortical contractility via physical interaction (i.e., contact) with actomyosin. That is, microtubule–F-actin colocalization has been observed directly in some systems (Sider *et al.*, 1999; Silverman-Gavrila and Forer, 2000). Furthermore, in a preliminary report, we have shown that F-actin is physically cleared from microtubule organizing centers in *Xenopus* egg extracts in a centrifugal manner that is similar to the displacement of F-actin away from repositioned GVs observed in the present study (Waterman-Storer *et al.*, 1998). In addition, Foe *et al.* (2000) recently proposed that myosin-2 is transported by microtubules away from centrosomes in *Drosophila* embryos; this transport would obviously be expected to reduce contractility in such regions.

Thus, microtubules negatively regulate contraction of the cortical actomyosin cytoskeleton in many systems and cortical flow in the oocyte system. As noted above, it is not clear whether or not our findings can be extrapolated to cortical flow during cytokinesis, and it should be noted that other work suggests that inhibition alone is insufficient to explain furrowing (reviewed by Rappaport, 1996; Rappaport, 1999). This raises the interesting possibility that the microtubule-dependent inhibition of actomyosin-based contraction observed here could be spatially coupled with a positive influence of specialized microtubule arrays on cortical actomyosin during cell division. For example, the spindle midzone, which is composed of antiparallel microtubules, has been shown to stimulate furrowing (Cao and Wang, 1996; Wheatley and Wang, 1996), implying that antiparallel microtubules might have a positive effect on actomyosin-based cortical contraction and cortical flow. It will be fascinating to directly measure the various positive and negative influences that distinct microtubule arrays have on actomyosin.

ACKNOWLEDGMENTS

We thank the members of our laboratory for helpful input throughout this study and Clare Waterman-Storer (Scripps Research Institute, La Jolla, CA) and Robert Adelstein (National Institutes of Health) for supplying key reagents. C.A.M. is a fellow of the Natural Sciences and Engineering Research Council of Canada. This work was supported by the National Science Foundation (MCB 9630860) and the National Institutes of Health (GM52932-01A2).

REFERENCES

Bement, W.M. (1992). Signal transduction by calcium and protein kinase C during egg activation. J. Exp. Zool. *263*, 382–397.

Bement, W.M., and Capco, D.G. (1989). Activators of protein kinase C trigger cortical granule exocytosis, cortical contraction, and cleavage furrow formation in *Xenopus laevis* oocytes and eggs. J. Cell Biol. *108*, 885–892.

Bement, W.M., Mandato, C.A., and Kirsch, M.N. (1999). Wound-induced assembly and closure of an actomyosin purse string in *Xenopus* oocytes. Curr. Biol. *9*, 579–587.

Bershadsky, A., Chausovsky, A., Becker, E., Lyubimova, A., and Geiger, B. (1996). Involvement of microtubules in the control of adhesion-dependent signal transduction. Curr. Biol. *6*, 1279–1289.

Bluemink, J.G. (1972). Cortical wound healing in the amphibian egg. J. Ultrastruct. Res. *41*, 95–114.

Bray, D., and White, J.G. (1988). Cortical flow in animal cells. Science *239*, 883–888.

Canman, J.C., and Bement, W.M. (1997). Microtubules suppress actomyosin-based cortical flow in *Xenopus* oocytes. J. Cell Sci. *110*, 1907–1917.

Cao, L.G., Fishkind, D.J., and Wang, Y.L. (1993). Localization and dynamics of nonfilamentous actin in cultured cells. J. Cell Biol. *123*, 173–181.

Cao, L.G., and Wang, Y.L. (1990). Mechanism of the formation of contractile ring in dividing cultured animal cells. II. Cortical movement of microinjected actin filaments. J. Cell Biol. *111*, 1905–1911.

Cao, L.G., and Wang, Y.L. (1996). Signals from the spindle midzone are required for the stimulation of cytokinesis in cultured epithelial cells. Mol. Biol. Cell *7*, 225–232.

Danilchik, M.V., Funk, W.C., Brown, E.E., and Larkin, K. (1998). Requirement for microtubules in new membrane formation during cytokinesis of *Xenopus* embryos. Dev. Biol. *194*, 47–60.

Danowski, B.A. (1989). Fibroblast contractility and actin organization are stimulated by microtubule inhibitors. J. Cell Sci. *93*, 255–266.

DeBiasio, R.L., LaRocca, G.M., Post, P.L., and Taylor, D.L. (1996). Myosin II transport, organization, and phosphorylation: evidence for cortical flow/solation-contraction coupling during cytokinesis and cell locomotion. Mol. Biol. Cell *7*, 1259–1282.

Drechsel, D.N., Hyman, A.A., Hall, A., and Glotzer, M. (1997). A requirement for Rho and Cdc42 during cytokinesis in *Xenopus* embryos. Curr. Biol. *7*, 12–23.

Fishkind, D.J., Silverman, J.D., and Wang, Y.L. (1996) Function of spindle microtubules in directing cortical movement and actin filament organization in dividing cultured cells. J. Cell Sci. *109*, 2041–2051.

Fishkind, D.J., and Wang, Y.L. (1995). New horizons for cytokinesis. Curr. Opin. Cell Biol. *7*, 23–31.

Foe, V.E., Field, C.M., and Odell, G.M. (2000). Microtubules and mitotic cycle phase modulate spatiotemporal distributions of F-actin and myosin-II in *Drosophila* syncytial blastoderm embryos. Development *127*, 1767–1787.

Gard, D.L. (1991). Organization, nucleation, and acetylation of microtubules in *Xenopus laevis* oocytes: a study by confocal immunofluorescence microscopy. Dev. Biol. *143*, 346–362.

Gard, D.L. (1993). Ectopic spindle assembly during maturation of *Xenopus* oocytes: evidence for functional polarization of the oocyte cortex. Dev. Biol. *159*, 298–310.

Gard, D.L., Cha, B.J., and Schroeder, M.M. (1995). Confocal immunofluorescence microscopy of microtubules, microtubule-associated proteins, and microtubule-organizing centers during amphibian oogenesis and early development. Curr. Top. Dev. Biol. *31*, 383–431.

Geuskens, M., and Tencer, R. (1979). An ultrastructural study of the effects of wheat germ agglutinin (WGA) on cell cortex organization during the first cleavage of *Xenopus laevis* eggs. I. Inhibition of furrow formation. J. Cell Sci. *37*, 47–58.

Gingell, D. (1970). Contractile responses at the surface of an amphibian egg. J. Embryol. Exp. Morphol. *23*, 583–609.

Hamilton, B.T., and Snyder, J.A. (1983). Acceleration of cytokinesis in PtK1 cells treated with microtubule inhibitors. Exp. Cell Res. *144*, 345–351.

Hird, S. (1996). Cortical actin movements during the first cell cycle of the *Caenorhabditis elegans* embryo. J. Cell Sci. *109*, 525–533.

Hird, S.N., and White, J.G. (1993). Cortical and cytoplasmic flow polarity in early embryonic cells of *Caenorhabditis elegans*. J. Cell Biol. *121*, 1343–1355.

Kimura, K., *et al.* (1996). Regulation of myosin phosphatase by Rho and Rho-associated kinase (Rho-kinase). Science *273*, 245–248.

Kolodney, M.S., and Elson, E.L. (1995). Contraction due to microtubule disruption is associated with increased phosphorylation of myosin regulatory light chain. Proc. Natl. Acad. Sci. USA *92*, 10252–10256.

Koppel, D.E., Oliver, J.M., and Berlin, R.D. (1982). Surface functions during mitosis. III. Quantitative analysis of ligand-receptor movement into the cleavage furrow: diffusion vs. flow. J. Cell Biol. *93*, 950–960.

Liu, B.P., Chrzanowska-Wodnicka, M., and Burridge, K. (1998). Microtubule depolymerization induces stress fibers, focal adhesions, and DNA synthesis via the GTP-binding protein Rho. Cell Adhes. Commun. *5*, 249–255.

Lyass, L.A., Bershadsky, A.D., Vasiliev, J.M., and Gelfand, I.M. (1988). Microtubule-dependent effect of phorbol ester on the contractility of cytoskeleton of cultured fibroblasts. Proc. Natl. Acad. Sci. USA *85*, 9538–9541.

Mandato, C.A., Benink, H.A., and Bement, W.M. (2000). Microtubule-actomyosin interactions in cortical flow and cytokinesis. Cell Motil. Cytoskeleton *45*, 87–92.

Merriam, R.W., and Christensen, K. (1983). A contractile ring-like mechanism in wound healing and soluble factors affecting structural stability in the cortex of *Xenopus* eggs and oocytes. J. Embryol. Exp. Morphol. *75*, 11–20.

Oegema, K., and Mitchison, T.J. (1997). Rappaport rules: cleavage furrow induction in animal cells. Proc. Natl. Acad. Sci. USA *94*, 4817–4820.

Rappaport, R. (1996). Cytokinesis in Animal Cells, Cambridge, UK: Cambridge University Press.

Rappaport, R. (1999). Absence of furrowing activity following regional cortical tension reduction in sand dollar blastomere and fertilized egg fragment surfaces. Dev. Growth Differ. *41*, 441–447.

Rappaport, R., and Rappaport, B.N. (1988). Reversing cytoplasmic flow in nucleated, constricted sand dollar eggs. J. Exp. Zool. *247*, 92–98.

Ren, X.D., Kiosses, W.B., and Schwartz, M.A. (1999). Regulation of the small GTP-binding protein Rho by cell adhesion and the cytoskeleton. EMBO J. *18*, 578–585.

Sanger, J.M., Dome, J.S., Hock, R.S., Mittal, B., and Sanger, J.W. (1994). Occurrence of fibers and their association with talin in the cleavage furrows of PtK2 cells. Cell. Motil. Cytoskeleton *27*, 26–40.

Schroeder, T.E. (1975). Dynamics of the contractile ring. In: Molecules and Cell Movement, ed. S. Inoue and R. Stephens, New York: Raven Press, 305–334.

Schroeder, T.E., and Strickland, D.L. (1974). Ionophore A23187, calcium and contractility in frog eggs. Exp. Cell Res. *83*, 139–142.

Scott, A.C. (1960). Surface changes during cell division. Biol. Bull. *119*, 260–272.

Shelton, C.A., Carter, J.C., Ellis, G.C., and Bowerman, B. (1999). The nonmuscle myosin regulatory light chain gene mlc-4 is required for cytokinesis, anterior-posterior polarity, and body morphology during *Caenorhabditis elegans* embryogenesis. J. Cell Biol. *146*, 439–451.

Sider, J.R., Mandato, C.A., Weber, K.L., Zandy, A.J., Beach, D., Finst, R.J., Skoble, J., and Bement, W.M. (1999). Direct observation of microtubule-F-actin interaction in cell free lysates. J. Cell Sci. *112*, 1947–1956.

Silverman-Gavrila, R.V., and Forer, A. (2000). Evidence that actin and myosin are involved in the poleward flux of tubulin in metaphase kinetochore microtubules of crane-fly spermatocytes. J. Cell Sci. *113*, 597–609.

Stith, B.J., Woronoff, K., Espinoza, R., and Smart, T. (1997). sn-1,2-Diacylglycerol and choline increase after fertilization in *Xenopus laevis*. Mol. Biol. Cell *8*, 755–765.

Taunton, J., Rowning, B.A., Coughlin, M.L., Wu, M., Moon, R.T., Mitchison, T.J., and Larabell, C.A. (2000). Actin-dependent propulsion of endosomes and lysosomes by recruitment of N-WASP. J. Cell Biol. *148*, 519–530.

Tencer, R. (1978). Transmembrane effects of lectins. I. Effects of wheat germ agglutinin and soybean agglutinin on furrow formation and cortical wound healing in *Xenopus laevis* eggs. Exp. Cell Res. *116*, 253–260.

Wang, Y.L., Silverman, J.D., and Cao, L.G. (1994). Single particle tracking of surface receptor movement during cell division. J. Cell Biol. *127*, 963–971.

Waterman-Storer, C.M., Salmon, E.D., and Bement, W.M. (1998). Microtubules modify actin networks in *Xenopus* egg extracts by dynein-dependent pushing and pulling of actin bundles. Mol. Biol. Cell *9*, 140a.

Wheatley, S.P., and Wang, Y. (1996). Midzone microtubule bundles are continuously required for cytokinesis in cultured epithelial cells. J. Cell Biol. *135*, 981–989.

White, J.G., and Borisy, G.G. (1983). On the mechanisms of cytokinesis in animal cells. J. Theor. Biol. *101*, 289–316.